Analysis of ac conduction in disordered solids

James Ross Macdonald
Department of Physics and Astronomy, University of North Carolina, Chapel Hill, North Carolina 27599-3255

(Received 5 December 1988; accepted for publication 22 February 1989)

Dyre [J. Appl. Phys. **64**, 2456 (1988)] has recently stated that the random free-energy barrier model of ac conduction in disordered solids, solved in the continuous time random-walk approximation with the effects of the maximum jump frequency eliminated, is quantitatively satisfactory in describing hopping conduction for a large number of solids. Here, predictions of this model, equivalent to the long-used box model, which posits a distribution of equally probable activation energies, are examined in depth, both without and with an upper cutoff. It is first demonstrated that the type of log-log plot on which Dyre appears to base his conclusion of quantitative adequacy does not allow adequate discrimination to be made between box-model predictions and those of other models, such as the Kohlrausch–Williams–Watts model, even when exact data are used. The results of numerous complex nonlinear least-squares fits of exact box-model data, and of such data containing substantial proportionally added random errors, to the box model, the WW model, the constant-phase-element model, and the Davidson–Cole [J. Chem. Phys. **19**, 1484 (1951)] response model make it clear that when using this fitting technique, one can identify the correct model, discriminate against incorrect ones, and obtain good parameter value estimates for the correct model. Further, when the highest frequency of the data exceeds the maximum jump frequency, its value can be accurately estimated. It is concluded that the case for the quantitative adequacy of the box model remains unproven. Future data fitting using complex nonlinear least squares should, however, allow a best-fit model to be selected unambiguously from those compared.

I. INTRODUCTION

The field of electrical conduction in disordered solids is an important and growing one. It is therefore timely and useful that Dyre[1] has recently reviewed work on the random free-energy barrier model (RFEB) for ac conduction in such materials, including amorphous semiconductors, conducting polymers, and ionically conducting glasses. In his interesting and valuable paper he compares theoretical solutions of the RFEB model using the continuous time random-walk (CTRW) approximation and the effective medium approximation (EMA) and shows that they yield nearly identical results for the frequency dependence of the real part of the complex conductivity $\sigma'(\omega)$. For this reason, most attention is given to the simpler hopping CTRW solutions and its predictions. Dyre concludes that it predicts all qualitative features of ac conduction in disordered solids and that it also yields quantitatively satisfactory agreement when compared to experimental results for a large number of solids. Nevertheless, Dyre rejects the possibility of quasiuniversality for the experimental results in the present field and points out the lack of quantitative agreement between the predictions of the RFEB model and some dielectric loss data. Because the physics underlying the RFEB model (and some of its generalizations) and the CTRW and EM approximations has been discussed by Dyre[1–4] and others,[5–10] the present work will be principally concerned with RFEB-CTRW frequency response predictions and their use in experimental analysis of ac response data.

Clearly, in carrying out the important task of identifying and quantifying the microscopic conduction parameters of disordered solids, it is of utmost importance to use the most applicable theory available to describe the conduction process. But which theory, of all those available, is the most applicable for a given situation? Dyre[1] has stated that because all disordered solids have similar ac properties, "only little can be learned about a solid from measuring its frequency-dependent conductivity." The learning, however, comes primarily not from the measuring but rather from the subsequent analysis and interpretation of the measurements. As Socrates might have said, "The inadequately examined dataset is not worth generating." Dyre's counsel of despair can perhaps be transformed to one of hope by replacing it by, "Inadequate analysis naturally leads to little, inadequate, or incorrect knowledge." But, is adequate analysis possible in the present area? An aim of the present paper is to demonstrate that it is. Perhaps such analysis will show that the similar properties mentioned by Dyre are largely consequences of analysis methods of inadequate power and discriminatory ability rather than of the underlying physical situation.

It is the thesis of the present paper that the quantitative agreement claimed by Dyre is not sufficiently justified and is thus an inadequate ground on which to base a conclusion as to the adequacy of the RFEB-CTRW model for describing the frequency response of disordered solids. As Dyre[1] points out, with only slight exaggeration, because "anything is a straight line in a log-log plot," one must take care in deducing power laws from apparently straight lines in log-log plots. Dyre's own comparisons are cast in the form of log-log plots of $\log[\sigma'(\omega)/\sigma(0)]$ vs $\log(\omega\tau)$, and one might generalize the above caution as, "many different models with two

 0021-8979/89/124845-09$02.40

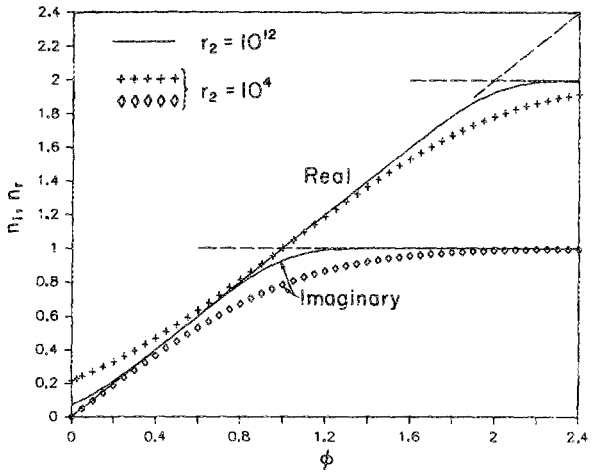

FIG. 1. Relations between the EDAE fractional-power, frequency-response exponents, n_r and n_i, and the basic EDAE exponent parameter ϕ for two different r values.

or three adjustable parameters can appear to fit ac response data for solids in such a log-log plot." But such appearances can be deceiving, and, in my opinion, conclusions based on them often represent a procrustean forcing of model predictions into an inappropriately sized bed. While reasonable or even good agreement between theory and experiment in such plots is of qualitative and illustrative interest, model adequacy conclusions should not be based on them.

Although the above thesis will be further justified in the rest of this paper, a few of its foundations are worth mentioning at this point. First, I agree with Dyre[1] that, "It should be emphasized that...results like Fig. 1 strongly suggest that any model for ac conduction should somehow be built on the assumption of a distribution of energy barriers." The RFEB model is needed so built, but it probably represents the simplest out of an infinite number of such possible models. It would be surprising indeed if nature, in its virtually infinite variety, limited itself to just this particular model for the ac response of disordered solids. Furthermore, there already exist many other different theoretical models for such conduction which lead to fractional exponential (Kohlrausch–Williams–Watts or WW) response,[11–13] often without the explicit inclusion of a distribution of energy barriers, or equivalently, a distribution of activation (or free) energies (DAE) (see Refs. 9, 14–16 for further references to such theories). And, of course, WW response is generally quite different from that of the RFEB model, yet it has been used to fit an appreciable amount of experimental data in the present area. Finally, log-log graphical comparison of only $\sigma'(\omega)$ omits examination of the response of the imaginary part of the complex conductivity, $\sigma''(\omega)$. Because of the ubiquitous presence of experimental errors, analysis of either the real or imaginary part is not equivalent to that of the other, even though they are connected holistically by the Kramers–Kronig relations. By using complex nonlinear least-squares (CNLS) fitting,[17] one can fit the full complex function at once, obtain useful estimates of the model parameter values and their uncertainties, and avoid the low resolution inherent in log-log plots.

Although no exact microscopic model exists which leads directly to a distribution of energy barriers and thus, to the RFEB or a more complex DAE model, such models fall, in some sense, between macroscopic and fully microscopic approaches, and, in the absence of exact N-body solutions, play a useful role. The distinguishing feature of the RFEB model is its assumption of equally likely free-energy barriers ranging from a minimum energy E_0 to a maximum E_∞. In the usual thermally activated situation, one has, for a typical relaxation time,

$$\tau = \tau_a \exp(E/k_B T). \tag{1}$$

This equation associates with E_0 and E_∞ the minimum and maximum relaxation time of the system, τ_0 and τ_∞, respectively. As before,[6–8] define their ratio r as $r \equiv \tau_\infty/\tau_0$, usually a large number. In a hopping model,[1] r is also the ratio of the maximum to the minimum hopping rate. As discussed elsewhere,[6,9,18] τ satisfies $0 < \tau_0 \leqslant \tau \leqslant \tau_\infty < \infty$. Thus, the RFEB model involves a continuous probability density function for E with a flat top and cutoffs at each end, and so is equivalent to the well-known box distribution. Dyre gives reference for this distribution going back to 1946. It i worth adding a bit of additional information. In fact, the box distribution was used in ferromagnetism in 1939,[19] in describing polymer response in 1948 and later,[20,21] in the dielectric response field from at least 1949 onwards,[22–24] and for photoconductors in 1951.[25] Furthermore, detailed consideration of the transient response of a dielectric system involving a single- or double-exponential DAE (and so including the box case) appeared in 1963,[5] and frequency response treatments applicable to both dielectric and conducting materials and involving these DAEs, as well as a Gaussian distribution, were published[6–8] in 1985 and 1987.

It was perhaps first pointed out by Fricke[26] that in aqueous electrolytes the real and imaginary parts of the experimental frequency response generally involve fractional-power frequency behavior. The ubiquity of such response has been emphasized by Jonscher,[27] particularly for solid dielectric materials, but it is found for amorphous semiconductors and solid electrolytes[28] as well. Thus, it necessarily appears, over at least a limited frquency range, in nearly all response theories (except the RFEB model). More specifically, if $\sigma(\omega) \equiv \sigma'(\omega) + i\sigma''(\omega)$, one finds that $\sigma'(\omega) \propto \omega^{n_r}$ and $\sigma''(\omega) \propto \omega^{n_i}$, again over a limited but possibly wide frequency range. Here, the real and imaginary part fractional exponents, which are often equal or nearly equal, satisfy $0 < n \leqslant 1$. Because such behavior is do endemic, it would clearly be desirable for the RFEB model to yield it. Although as Dyre[1] points out, there is no exact power-law response present in RFEB-CTRW model predictions, it turns out that expansion for $\omega\tau \gg 1$, where Dyre's τ is the present τ_∞, yields $n_r \simeq 1 - 2/\ln(\omega\tau)$, a somewhat frequency-dependent fractional exponent. For $10^2 \leqslant (\omega\tau) \leqslant 10^9$, where 10^9 is the upper limit of the data presented by Dyre, this expression yields a n_r varying from about 0.57 to 0.91. Such frequency-dependent variation is rarely, if ever, apparent in the actual σ' data, but, if present, may be obscured by unavoidable errors in the data and the widespread use of log-log plotting. Furthermore, actual reported exponents are generally not taken to

be frequency dependent but often are found to be essentially constant over many decades of frequency. To my knowledge, there have, in fact, been no unambiguous comparisons between RFEB predictions and data for disordered solid which confirm this model as the best-fitting choice. Again, part of the problem arises from data errors, but another part is associated with the acceptance of model-fitting decisions based on the use of graphical comparisons rather than on more powerful procedures.

The above conclusions is not meant to rule out the possibility that some real data may be most appropriately fitted by the RFEB model, but instead to suggest that the case for this model remains unproven thus far. Furthermore, since both the WW and more general DAE models, such as the exponential distribution of activation energies (EDAE) model, directly yield fractional exponents which may be frequency independent over a wide range and whose possible values fall in the full range $0<n\leqslant 1$, it seems inappropriate to try to force the RFEB model to yield approximate fractional exponents to save the model.

II. BACKGROUND: THE EDAE$_1$ AND RFEB-BOX-DISTRIBUTION MODEL RESPONSE FUNCTIONS

Experimental measurements in the present impedance spectroscopy[28] area usually result in values of the impedance, $Z(\omega)=Z'(\omega)+iZ''(\omega)$, or its inverse, the admittance, $Y(\omega)\equiv[Z(\omega)]^{-1}=Y'(\omega)+iY''(\omega)$. Two other response functions are often of interest, the complex dielectric constant, $\epsilon(\omega)=\epsilon'(\omega)-i\epsilon''(\omega)$, and its inverse, the complex modulus function, $M(\omega)=M'(\omega)+iM''(\omega)$, probably first considered by Schrama.[29] Let us define the capacitance of the empty measuring cell as C_c, a quantity which involves the vacuum permittivity ϵ_v. Then, $\epsilon(\omega)\equiv Y(\omega)/(i\omega C_c)$. But for the materials considered here, the dc or low-frequency limit of $Y(\omega)$, the conductance $Y'(0)\equiv G(0)$, is not zero, and its leads to a possibly undesirable term in $\epsilon(\omega)$ given by $G(0)/(i\omega C_c)\equiv\sigma(0)/(i\omega\epsilon_v)$. Here, $\sigma(0)\equiv\sigma'(0)$ is the low-frequency limiting value of the real part of $\sigma(\omega)\equiv Y(\omega)/(C_c/\epsilon_v)$, the complex conductivity.

For plotting dielectric constant results in the complex dielectric constant plane when $G(0)\neq 0$, it is customary to consider a modified dielectric constant $\epsilon_m(\omega)$, defined as

$$\epsilon_m(\omega)\equiv[Y(\omega)-G(0)]/(i\omega C_c), \tag{2}$$

provided that the effect of any nonzero $\epsilon_m(\infty)\equiv\epsilon(\infty)$ is included in $Y(\omega)$; see discussion below. It is also then convenient to define the dielectric strength parameter as $\Delta\epsilon\equiv[\epsilon_m(0)-\epsilon(0)]$. The above subtraction of the $G(0)$ term keeps $\epsilon_m''(\omega)$ from approaching infinity as $\omega\to 0$; the transformation from $\epsilon(\omega)$ to $\epsilon_m(\omega)$ is unnecessary, however, if one deals with $M(\omega)$ [or $Z(\omega)$ or $Y(\omega)$] rather than $\epsilon(\omega)$, or if one is concerned only with CNLS fitting. Furthermore, although there is no problem in subtracting $G(0)$ from a theoretical expression for $Y(\omega)$, the subtraction of a $G(0)$, itself derived from experiment, from experimental data in order to obtain values of $\epsilon_m(\omega)$ will, necessarily, introduce some error in the result because of the uncertainty in the estimated value of $G(0)$.

With this background, let us now consider the detailed response of the RFEB, or box-distribution model. It is instructive to start with the single-exponential distribution of the activation energies model, the EDAE$_1$, more general than the box model. In normalized terms, one finds,[6-8] for $\phi_j\neq 0$,

$$I_j(\Omega,\phi_j)=\left(\frac{\phi_j}{1-r^{-\phi_j}}\right)\int_0^{y_0}\left(\frac{\exp(-\phi_j y)dy}{[1+i\Omega\exp(-y)]}\right) \tag{3}$$

where $\Omega\equiv\omega\tau_\infty$, $y_0\equiv\ln(r)$, and ϕ_j, which satisfies $-\infty<\phi_j<\infty$, is a characteristic exponent of the theory; it depends on the strength factor of the exponential distribution. When ϕ_j is unity, the exponential distribution reduces to the box distribution. The integral cannot be expressed in simple closed form for arbitrary values of ϕ_j, but can be[6] for various integral and fractional values of ϕ_j. Although it can be written as a hypergeometric function, it has been found easier to evaluate it by numerical integration when it is needed in the general and powerful CNLS fitting program[17] available at nominal cost from the author's department.

The subscript j appearing in the above can be either C or D, designating either an intrinsically conductive or an intrinsically dielectric situation, since the same normalized response function can represent either one.[6] Here, we shall eventually be dealing with a conductive situation, but it will be useful to maintain the generality of the j subscript for a bit longer. The normalized immittance function $I_j(\Omega,\phi_j)$ is defined as

$$I_j(\Omega,\phi_j)\equiv[U_j(\omega)-U_j(\infty)]/[U_j(0)-U_j(\infty)], \tag{4}$$

where $U_C(\omega)\equiv Z(\omega)$ and $U_D(\omega)\equiv\epsilon(\omega)$. In the present conductive situation, $I_C(\Omega,\phi_C)$ is thus a normalized impedance response function, and when electrode-interface resistance is negligible, we have $U_C(\infty)=0$ and $U_C(0)=Z'(0)\equiv R(0)\equiv[G(0)]^{-1}$.

For the REFB box-distribution situation, one sets $\phi_j=1$ in Eq. (3) and integration leads to[6]

$$I_j(\Omega,1)=[i\Omega(1-r^{-1})]^{-1}\ln[(1+i\Omega)/(1+i\Omega r^{-1})], \tag{5}$$

a result in agreement with that of Dyre[1,2] and with the earlier box-distribution treatments already cited. Also of interest (since its real part is the quantity primarily considered by Dyre) is the normalized admittance[6] or complex conductivity, $S_j(\Omega,1)\equiv[I_j(\Omega,1)]^{-1}$, here equal to $[Y(\omega)/G(0)]=[\sigma(\omega)/\sigma(0)]$. Now Dyre has suggested that one should try to eliminate completely all the effects of the maximum jump frequency (here, equivalent to the minimum relaxation time τ_0). To do so, he effectively lets $r\to\infty$, leading to the simple result

$$S_{C\infty}(\Omega,1)=i\Omega/\ln(1+i\Omega). \tag{6}$$

Unfortunately, the RFEB-CTRW model leads to an expression for $\sigma(0)$ which goes to infinity as $r\to\infty$. This infinite-conductivity catastrophe is an illustration of the nonphysical character of the $r\to\infty$ assumption.[6,9,18] To avoid its implications and still use Eq. (6) as an appropriate fitting model, Dyre[1] takes $\sigma(0)$ a a free-fitting parameter (as, in fact, we do here as well), since, in real conducting situations, it is not infinite. In fitting actual data, the fitting results themselves

can be used to determine whether or not the $r = \infty$ approximation is appropriate and adequate, rather than prejudging the matter. But note that even with a finite $\sigma(0)$, Eq. (6), but not Eq. (5), leads to infinite conductivity as $\omega \to \infty$, a further nonphysical result, although one not fully amenable to experimental test!

III. SOME FITTING RESULTS FOR THE $r = \infty$ BOX-DISTRIBUTION RESPONSE FUNCTIONS

Plots of the normalized response functions $I_j(\Omega,\phi_j)$ and $S_j(\Omega,\phi_j)$ associated with Eq. (3) have been given[6] earlier for a variety of finite r values and many ϕ_j's, including $\phi_j = 1$, the box DAE. Because of Dyre's claims of quantitative agreement with experiment of the simple $r = \infty$, $\phi_C = 1$ expression of Eq. (6) for conductive situations in disordered solids, it is worthwhile to carry out some CNLS fitting comparisons with the predictions of this response model. This will first be done omitting any $\epsilon(\infty)$ effects; later their influence will be included explicitly.

Equation (6) leads, for the present conductive situation, to

$$Y_\infty(\omega) = i\omega\tau_\infty G(0)/\ln(1 + i\omega\tau_\infty), \qquad (6')$$

and

$$Z_\infty(\omega) = R(0)[\ln(1 + i\omega\tau_\infty)]/(i\omega\tau_\infty). \qquad (7)$$

There are two parameters in these equations, the scale factor $G(0)$ or $R(0)$, and the maximum relaxation time, τ_∞. Although, we have elected here and in the following to deal with admittance rather than with complex conductivity, since admittance may be measured directly, the results obtained are not affected by this choice. We first ask how well exact "data" calculated from these expressions can be fitted by two other different but important distributed response models: Williams–Watts (WW), and constant phase element (CPE).[30] Since the real and imaginary WW frequency response functions cannot be expressed in closed algebraic form and are very difficult to evaluate directly as integrals, an accurate approximation for them was developed[31] and incorporated in the CNLS fitting program mentioned above. The expression used for CPE response at the Y level is just $(i\omega\tau_0)^{\psi_c}$. There are three free parameters in a WW fit: P_1, the scale parameter; P_2, a WW relaxation time τ_W; and P_3, the WW fractional exponent ψ_W. Only the parameters $P_2 \equiv \tau_c$ and $P_3 \equiv \psi_c$ are present in a CPE fitting.

Before discussing fits of the WW and CPE models to the predictions of the $r = \infty$ box-distribution model, it is worthwhile considering some earlier but relevant results[8] for the general EDAE of Eq. (3), $I_j(\Omega,\phi_j)$. In Fig. 1, the fractional frequency response exponents n_r and n_i are plotted as a function of the EDAE ϕ (here ϕ_j) for two different values of r. These values apply to regions of $I_j(\Omega,\phi_j)$ response where constant-exponent behavior is an excellent approximation. The curves show that although ϕ may readily exceed unity, n_i does not.

For simplicity in comparisons, the values of the parameters in Eqs. (6) and (7) were set to unity, and data were calculated over an appreciable range of Ω. Again for simplicity, we shall omit parameter and data units herein. Data sets

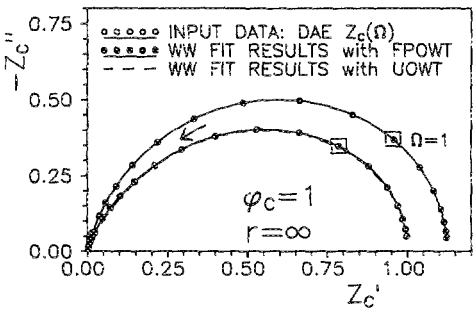

FIG. 2. Impedance-plane plots of CNLS fitting results, for proportional and unity weighting, of the Williams–Watts model to exact data calculated from the box-distribution model with $r = \infty$. The points where the normalized frequency Ω is unity are indicated.

were generated from the above equations for the range of Ω used by Dyre for some of his data-model comparisons: $0.1 \leqslant \Omega \leqslant 10^6$. For WW fitting there were 43 Ω values, distributed uniformly on a logarithmic scale with 6 points/decade. But, CPE response, which leads to a constant slope of the real and imaginary parts of a response function on a log-log plot, is only appropriate for the approximate straight-line part of log-log Dyre box response. To obtain an approximate fractional exponent, Dyre himself used the range $10^3 \leqslant \Omega \leqslant 10^6$ and found a value of about 0.8. We shall thus fit the CPE only to this part of the Eq. (6') data, the top 19 points of the full range. It is worth noting that although we shall use $\Omega \equiv \omega\tau_\infty$ as the frequency variable of the exact data, the related quantity $\omega\tau_W$, where τ_W is obtained from WW fitting, is generally unequal to Ω.

The results of many different fits appear in Figs. 2–4 and in Table I. Although these results are largely self explanatory, a few additional definitions are needed. The fit-type choice C indicates CNLS fitting of a complex function; R designates nonlinear least-squares (NLSQ) fitting of the real part only; and I applies for NLSQ fitting of the imaginary part only. Two basic types of data weighting[17] have been used in the fits: unity weighting (U or UWT) and proportional weighting (P or PWT). For PWT the uncertainties used in calculating the weights are taken proportional to

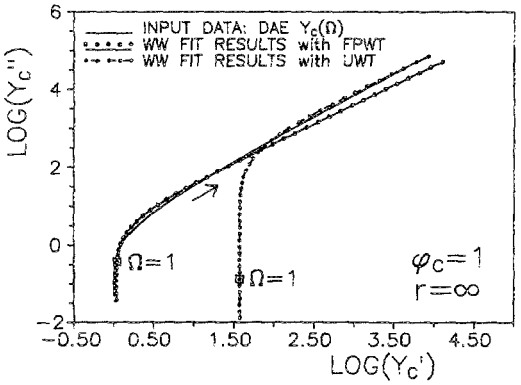

FIG. 3. Admittance-plane plots of CNLS fitting results, for proportional and unity weighting, of the Williams–Watts model to exact data, calculated from the box-distribution model with $r = \infty$.

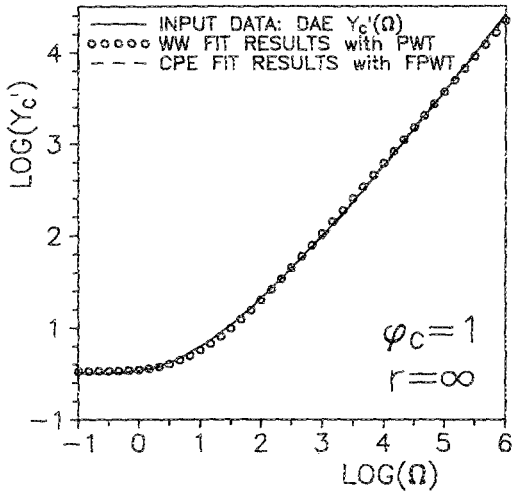

FIG. 4. Logarithm of the real part of the admittance, the conductance, vs the logarithm of normalized frequency. Results are shown for NLSQ fitting with proportional weighting of both the Williams–Watts model and the constant-phase element model to exact data calculated from the box-distribution model with $r = \infty$.

the individual real or imaginary data values, while they are taken unity for UWT. Thus, PWT is appropriate when the random errors in the data are a constant percentage of the data values themselves. Then, all data points are important in the fitting, the very large as well as the very small, but for UWT only the largest values dominate.

Function-proportional weighting (FP or FPWT) is just like PWT except predicted function values rather than data values are used in calculating the weights. It should be emphasized that if the actual errors in experimental measurements involve a random distribution having zero mean which is multiplied by a constant fraction of the absolute values of the true error-free model predictions (exact data values), then, this is the often expected situation of constant precentage errors. If the correct response model is fitted to data containing such errors, then FPWT and not PWT is the appropriate weighting choice. Unpublished Monte Carlo results of the author show that in such conditions FPWT leads to very much smaller bias in parameter estimates than does PWT. The final type of weighting listed in Table I involves the letter O, standing for optimization. It is only appropriate for complex fitting, is applied after UWT, PWT, or FPWT has been used, and involves iterative adjustments to all real-part weights and to all imaginary-part weights designed to lead to equal contributions of the real and imaginary fit standard deviations to the overall standard deviation of the fit. The final result is that whichever part originally fits worst contributes less to the final fit and thus to the parameter estimates, and vice versa. FPWT and optimization have not been described previously in the present context but often prove very useful. In this paper, the decision was made to present only fitting results for the kind of weighting (U or UO, or P, FP, or FPO) which led to the smallest parameter estimated standard deviations for each particular type of fit. Although the differences found with different P or U types of

TABLE I. CNLS fitting results for $\phi_i = 1$, $r = \infty$ DAE model "data." For the WW fitting model, $0.1 \leqslant \Omega \leqslant 10^6$, while for the CPE, $10^3 \leqslant \Omega \leqslant 10^6$.

Fit model	Data form	Fit type	WT	S_f	P_1	P_2	P_3
WW	Y_C	C	FP	0.203	0.942|6.1×10^{-2}	0.323|8.3×10^{-2}	0.848|6.6×10^{-3}
			U	56.1	0.027|2.6×10^{-1}	0.003|2.8×10^{-1}	0.926|3.9×10^{-4}
		I	FP	0.100	0.733|6.9×10^{-1}	0.353|7.8×10^{-1}	0.858|4.5×10^{-3}
			U	27.4	1.46|524	0.261|567	0.924|6.0×10^{-4}
		R	P	6.6×10^{-2}	0.955|2.2×10^{-2}	0.302|4.3×10^{-2}	0.774|5.9×10^{-3}
		U		7.12	1.70|2.3×10^{-1}	0.026|2.8×10^{-1}	0.845|1.4×10^{-3}
	Z_C	C	FPO	0.201	1.125|2.2×10^{-2}	0.370|2.8×10^{-2}	0.868|4.3×10^{-3}
			UO	1.3	1.001|6×10^{-4}	0.430|1.6×10^{-3}	0.773|1.1×10^{-3}
		I	FP	0.103	1.081|2.3×10^{-2}	0.390|3.0×10^{-2}	0.852|5.5×10^{-3}
			U	8.3×10^{-4}	1.004|1.0×10^{-3}	0.429|1.7×10^{-3}	0.769|1.5×10^{-3}
		R	FP	0.230	0.878|8.0×10^{-2}	0.208|1.1×10^{-1}	0.894|6.0×10^{-3}
			U	1.5×10^{-3}	1.000|8×10^{-4}	0.430|2.7×10^{-3}	0.775|1.8×10^{-3}
CPE	Y_C	C	FPO	0.110	⋯	0.225|1.8×10^{-2}	0.905|1.9×10^{-3}
			U	92.6	⋯	0.177|7.1×10^{-3}	0.926|6.0×10^{-4}
		I	P	1.7×10^{-2}	⋯	0.223|2.0×10^{-2}	0.906|2.1×10^{-3}
			U	41.5	⋯	0.179|1.0×10^{-2}	0.924|8.4×10^{-4}
		R	FP	3.8×10^{-2}	⋯	0.290|2.4×10^{-2}	0.807|5.2×10^{-3}
			U	12.8	⋯	0.227|1.2×10^{-2}	0.845|2.2×10^{-3}
	Z_C	C	FPO	0.120	⋯	0.234|2.0×10^{-2}	0.902|2.2×10^{-3}
			UO	2.6×10^{-5}	⋯	0.298|1.0×10^{-2}	0.869|1.8×10^{-3}
		I	P	2.1×10^{-2}	⋯	0.236|2.2×10^{-2}	0.901|2.5×10^{-3}
			U	1.1×10^{-5}	⋯	0.292|1.3×10^{-2}	0.872|2.2×10^{-3}
		R	FP	1.1×10^{-4}	⋯	6.3×10^{-5}|2.0×10^{-1}	0.9999|1.2×10^{-5}
			U	2.8×10^{-8}	⋯	3.2×70^{-4}|8.1×10^{-2}	0.9999|2.6×10^{-5}

weighting were often small, they were sometimes appreciable. Finally, notice that results are presented in this section only for $Y(\Omega)$ and $Z(\Omega)$, not for $\epsilon(\Omega)$ and $M(\Omega)$. Although this decision was made partly to save space, more importantly, it turns out[17] that CNLS fits of $Y(\Omega)$ and $\epsilon(\Omega)$ for any P-type (but not U-type) weighting yield exactly the same results, as do such fits of $Z(\Omega)$ and $M(\Omega)$.

The quantity S_f in Table I is the estimated standard deviation of the overall fit. Its values for the fits involving UWT may be compared, as may those involving any type of PWT, but the S_f's for the two different weighting types are not comparable. The parameter estimates are presented in the form $A\,|B$, where A is the parameter value estimate and B is its relative standard deviation estimate, sometimes called the coefficient of variation. When B is of the order of 0.5 or greater, the parameter value involved is poorly determined.

Figures 2 and 3 present complex plane plots of Z_C and Y_C which compare CNLS WW-fit results with the original data calculated from Eqs. (6′) and (7). The original data points are shown explicitly in Fig. 2; the $\Omega = 1$ point is identified; and the curves were plotted with spline fitting between points to avoid the straight lines which would otherwise connect adjacent points. The arrows show the direction of increasing frequency. Note that the FPOWT WW curve of Fig. 2 is quite far from the original data while the UOWT curve seems to indicate an almost perfect fit. Certainly, these results indicate that one would be entirely unable to distinguish between the RFEB box model and the WW model on the basis of this UOWT fit. Such discrimination would be even more difficult, of course, for real data containing measurement errors. But the situation is quite different when one carries out a fit of the data at the Y level. Figure 3 shows results for such fitting in a log-log complex plane plot. For this plot it is the FPWT curve, rather than the UWT one, which seems to agree better with the data. But remember the earlier strictures about log-log plots! Note that the UWT result, while agreeing appreciably better with the data at high Ω, is hopeless at low Ω values because with this weighting the fit is essentially determined only by the region where the data magnitudes are large. These results indicate that unless actual experimental data had very large errors indeed, one could certainly distinguish between the two models. Model discrimination is further discussed and illustrated in Sec. IV.

Finally, Fig. 4 presents a log-log plot of the kind used by Dyre and others in the past. Since past comparisons of models and data in the present area have not usually involved the imaginary part of the data at all, we show here the results of NLSQ fits of the real part only. We see that even with good data one would not be able to distinguish, on the basis of such a plot alone, between the RFEB and the WW models. Furthermore, the dashed CPE fit results, present only at the higher frequencies, are virtually indistinguishable on the log-log plot from the (exact) data. These results show why it was reasonable, on the basis of plots like these, for Dyre to claim quantitative agreement between theory and experiment. Hopefully, the present analysis should convince the reader that such a conclusion should not be based solely on comparisons of this type.

The foregoing plots are all consistent, of course, with the quantitative fitting results listed in Table I, but this table includes many fits not plotted. What conclusions can we draw from these fit results? First, that U and P weighting can lead to appreciably different results for parameter estimates when an inappropriate model is fitted to the data. Second, that Y and Z fits, even with the same weighting type, can also yield appreciably different results here. These systematic error differences are immediate and important signs that one is fitting the wrong model to the data. Fitting the right model, even with realistic data containing random errors, would lead to smaller differences and to a much more consistent overall picture. Some results of such fitting are presented in the next section.

Three specific results included in the table are worth particular mention. First, note that although most of the P_1 scale factor estimates are close to the RFEB value of unity, none of the P_2 time constant estimates are close to the RFEB τ_∞ input value of unity. This is not surprisingly since τ_W and τ_c apply to different models than does the present τ_∞, and thus they are not fully comparable. Next, note that the real-part FPWT CPE fit at the Y level yields a value of the fractional exponent ψ_c of about 0.81, close to the value of 0.8 found by Dyre for the same fitting region. But note all the other estimates of ψ_c and ψ_W listed in the table, ones different from 0.8. Again, their variation arises from fitting the wrong model to data, data which in fact do not involve a constant power-law fractional exponent at all. In procrustean fashion, the CNLS and NLSQ fits do their best to match wrong models to the data but at the expense of consistency. Finally, note the last I and R ψ_c results in the table, those for CPE fitting at the Z level. These values, particularly those for P weighting, yield the individual slopes of the imaginary and real response curves in log(real) or log(imaginary) vs log(frquency) plots and should be compared with the n_i and n_r, $\phi = 1$ values shown in Fig. 1. Although there $r = 10^4$ or 10^{12} and here $r = 10^8$, we see that agreement is excellent, as it should be since the same quantities are being compared. Note, however, that Fig. 1 shows the pertinent relations between n_i and n_r and ϕ not just for the present $\phi = 1$ but for a large range of ϕ values.

IV. COMPARISONS AND FITS FOR NONZERO $\epsilon(\infty)$

Dyre[1] has argued that data in the present field should be presented in terms of $\sigma'(\omega)$ rather than $M(\omega)$ because the latter [and $Y(\omega)$, $Z(\omega)$, and $\epsilon_m(\omega)$ as well] mixes in the effect of a high-frequency dielectric constant ϵ_∞ associated with atomic polarizability, while its effects do not appear in $\sigma'(\omega)$. Let us consider the matter in more detail and move toward a more realistic model of real data. Certainly real IS data always involves capacitative response associated with the geometrical capacitance of the bulk material between electrodes, even when there is no distribution of activation energies present and/or the material is nonconducting. This bulk capacitance, $C_B \equiv \epsilon_B C_c$, neglected thus far in the present work, is frequency independent in the usual experimental frequency range and appears in parallel with an admittance circuit element arising from any dispersion process

present. When it is included in the response, Eqs. (2), (4), and (5) lead to

$$\epsilon_m(\Omega) = \epsilon_B + (\{(1-r^{-1})/\ln[(1+i\Omega)/(1+i\Omega r^{-1})]\} - (i\Omega)^{-1})\,H, \quad (8)$$

where

$$H \equiv [\tau_\infty G(0)/C_c] \equiv [\tau_\infty \sigma(0)/\epsilon_v]\,. \quad (9)$$

We have, for simplicity, omitted the $j = C$ subscript and will do so hereafter. The expression for $\epsilon(\Omega)$ is the same as that of Eq. (8) except the $(i\Omega)^{-1}$ term does not appear. It follows from Eq. (8) that

$$\epsilon_m(0) = \epsilon_B + [(1+r^{-1})/2]H, \quad (10)$$

and

$$\epsilon(\infty) = \epsilon_B + [(1-r^{-1})/\ln(r)]H. \quad (11)$$

Thus, when $r < \infty$, as it always is in reality, there is an additional contribution to $\epsilon(\infty)$ beyond that associated with ϵ_B. The dielectric strength parameter is then

$$\Delta\epsilon = \{[(1+r^{-1})/2] - [(1-r^{-1})/\ln(r)]\}\,H. \quad (12)$$

Note that $\Delta\epsilon \to 0$ as $r \to 1$ as it should, and that it approaches[1] $H/2$ as $r \to \infty$. Because of the presence of the $\ln(r)$ term, however, the result is not very well approximated by $H/2$ even for r values as large as 10.[30]

It is now of interest to express such quantities as $\epsilon(\Omega)$ and $M(\Omega)$ in terms of $\Delta\epsilon$ rather than H, since there exist appreciable data for the $\Delta\epsilon$s of ionically conducting glasses (see citations in Ref. 1). Let us define $D \equiv \Delta\epsilon/\epsilon_B$, a quantity which usually falls in the range of about 0.2–30 or so, and

$$f(r) \equiv \ln(r)/\{[(1+r^{-1})/(1-r^{-1})]\,[\ln(r)/2] - 1\}, \quad (13)$$

where $f(\infty) = 2$. Then we may write

$$\epsilon_m(\Omega)/\epsilon_B = 1 + Df(r)(\{1/\ln[(1+i\Omega)/(1+i\Omega r^{-1})]\} - \{1/i\Omega(1-r^{-1})\})\,, \quad (14)$$

and

$$\epsilon_B M(\Omega) = \{1 + (Df(r)/\ln[(1+i\Omega)/(1+i\Omega r^{-1})]\}^{-1}. \quad (15)$$

For plotting purposes it is convenient to define some normalized quantities. Let $[(\epsilon_m(\Omega) - \epsilon_B)/\epsilon_B] \equiv \epsilon_d(\Omega)$; define $\epsilon_{d\infty}(0)$ as the value of $\epsilon_d(0)$ for $r = \infty$; and let $\epsilon_{mN}(\Omega) \equiv \epsilon_d(\Omega)/\epsilon_{d\infty}(0)$, a quantity independent of D. Note that $M(0) = 0$ and $M(\infty) = \epsilon_B^{-1}\{1 + [Df(r)/\ln(r)]\}^{-1}$. Next, define $M_N(\Omega) \equiv M(\Omega)/M(\infty)$. It follows from the earlier definitions that $(C_B/\tau_\infty)Z(\Omega) = \epsilon_B M(\Omega)/i\Omega$. Now $(C_B/\tau_\infty)Z(0) = [Df(r)/(1-r^{-1})]^{-1}$ and we may define the normalized impedance as $Z_N(\Omega) \equiv Z(\Omega)/Z(0)$. Finally, when $\epsilon_B = 0$, it is helpful to consider $M_n(\Omega) \equiv HM(\Omega)$.

In order to compare $\epsilon_B \neq 0$ with $\epsilon_B = 0$ results, I first present in Fig. 5 a three-dimensional (3D) perspective plot[32] of $M_n(\Omega)$ for two different r values. This type of plot shows 3D curves and, as well, their projections in the three coordinate planes; thus all types of response curves are included. Here, as usual, $0.1 \leqslant \Omega \leqslant 10^6$ for both sets of data, and the tic marks on the real and imaginary axes are 1.4 apart, while

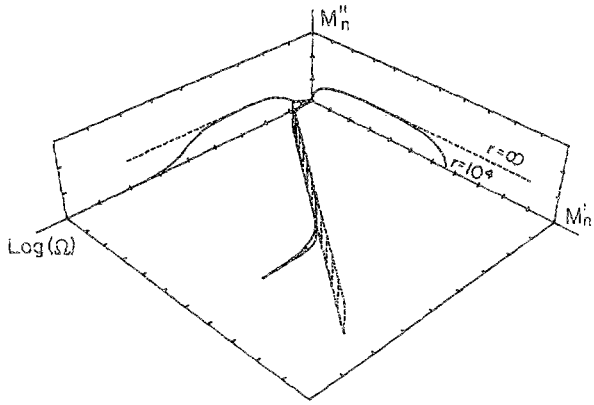

FIG. 5. 3D perspective plot, and its three projections, of exact, normalized, complex modulus data, $M_n(\Omega)$, for the box-distribution model with $r = 10^4$ and $r = \infty$. Here, $\epsilon_B = 0$.

those on the log frequency axis are 1.0 apart. These results show one very significant feature: namely, that there are extended flat parts of the curves, regions where $M''(\Omega) = \pi/2H$, a frequency-independent value. This is an important characteristic signature of box-distribution response and would be much easier to identify than the appearance of a frequency-dependent fractional exponent as in Dyre's approach. Unfortunately, matters are more complicated because ϵ_B is never zero.

Figures 6, 7, and 8 show complex plane response plots for the more realistic $\epsilon_B \neq 0$ situation for two r value and two typical D values. Although the $r = 10^4$, $D = 20$ curve of the $M_N(\Omega)$ response of Fig. 6 does show a flat region like that of Fig. 5, such regions only appear for large D. Note that there are enough differences here between the curves with the same D values but different r ones to suggest that one should be able to determine the values of r if the present model applies. Incidentally, for the $r = 10^4$ curves $0.01 \leqslant \Omega \leqslant 10^5$, but since the $r = \infty$ curves do not reach their limiting high-frequency value until $\Omega = \infty$, we have used the much larger range $0.01 \leqslant \Omega \leqslant 10^{14}$ for them in all three figures.

The Z_N results of Fig. 7, where only the low-frequency part of the full frequency response is resolved, show little effect of different r values, unlike the M_n results, where the

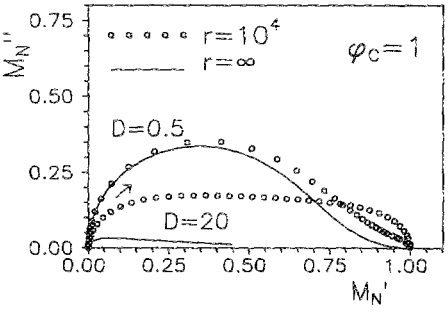

FIG. 6. Complex plane plots of exact, normalized, complex modulus data $M_N(\Omega)$ for the box-distribution model with $r = 10^4$ and $r = \infty$ for $D \equiv \Delta\epsilon/\epsilon_B$ values of 0.5 and 20.

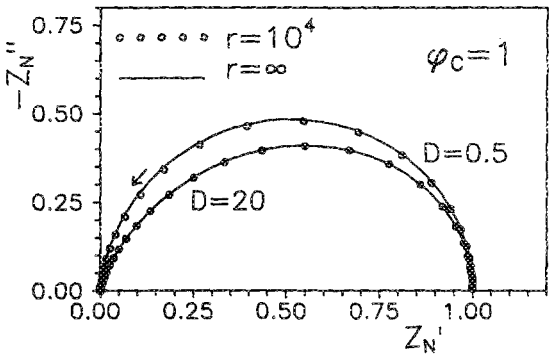

FIG. 7. Complex plane plots of exact, normalized, impedance data $Z_N(\Omega)$, for the box-distribution model with $r = 10^4$ and $r = \infty$ for D values of 0.5 and 20.

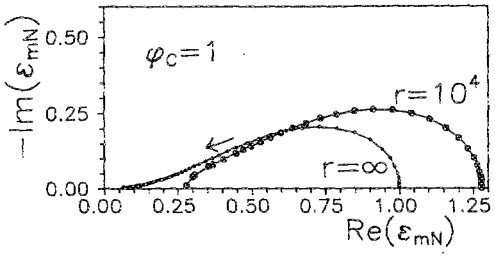

FIG. 8. Complex plane plots of exact, normalized, modified complex dielectric constant data, $\epsilon_{mN}(\Omega)$, for the box-distribution model with $r = 10^4$ and $r = \infty$. With the normalization used, the results are independent of the value of ϵ_B.

higher-frequency part of the response is emphasized. It should be remembered, however, that although M and Z curves will have different shapes, as will Y and ϵ ones, the members of these pairs will lead to exactly the same parameter estimates when any type of PWT is used in CNLS fitting. Finally, the ϵ_{MN} curves of Fig. 8, which are independent of D because of the normalization used, do show an appreciable dependence on r even if they are translated to have the same zero-frequency limiting value. Note that for all curves with $r < \infty$ the final approach to the real axis at high and low frequencies is vertical, as it should be[18] for physically realistic response.

The foregoing results suggest that it would be of considerable interest for experimental data analysis in the present field to examine just how well CNLS fitting can yield good parameter estimates for real data associated with the present RFEB-CTRW box-distribution model and whether one can distinguish it from other response models. To simulate such real data, I first calculated an exact $Y(\omega)$ data set of 73 points, extending over the range $0.01 \leqslant \Omega \leqslant 10^{10}$. The finite-size, box-distribution expression for $Y_C(\omega)$ was cast in the form

$$Y_C(\omega) = (i\omega C_B) + G(0)\{i\omega\tau_\infty(1 - r^{-1})/\ln[(1 + i\omega\tau_\infty)/(1 + i\omega\tau_\infty r^{-1})]\} \quad (16)$$

for the calculation of the data. For such calculation, $G(0)$ and τ_∞ were each set equal to unity, with negligible loss of generality, and r was taken as 10^8. Because of the relation $D = (\tau_\infty G(0)/C_B)[(1 - r^{-1})/f(r)]$, one can readily calculate D (and $\Delta\epsilon$) given values of the other quantities. In order to have $D = 1$, C_B must equal about 0.445 713 for the present parameter value choices, and this value was used in generating the exact data. Next, random errors were added proportionately to the exact data. To do so, first two sets of 73 independent (pseudo) random numbers were constructed, each drawn from a normal distribution having zero mean and a nominal standard deviation σ_r of 0.05. One set was added proportionately, point by point, to the real part of the exact data and the other to the imaginary part. The choice of 0.05 was made in order that the resulting data be of average quality, neither very good nor very bad. To examine the effects of using data of more limited frequency range, the first 49 points of the above $Y(\omega)$ dataset, involving the range $0.01 \leqslant \Omega \leqslant 10^6$, were also used in the fitting.

In the CNLS fitting, the program uses the integral of Eq.

TABLE II. CNLS fitting results for $\phi_C = 1$, $r = 10^8$ DAE model data with $\sigma_r = 0.05$ random errors and nonzero parallel capacitance C_B chosen to yield $D = 1$.

Line no.	Data/form fit-WT	S_f	$R(0)$	τ_∞	$\ln(r)$	ϕ or ψ	C_B
1	Y_C-C-P	0.041	0.985|0.010	0.978|0.017	47.1|0.98	1.0	0.445|0.009
2	Y_C-C-P	0.041	0.986|0.011	0.983|0.043	43.6|1.7	1.006|0.043	0.442|0.052
3	Y_C-C-FPO	0.045	0.984|0.010	0.977|0.016	18.38|0.001	1.0	0.446|0.008
4	Y_C-C-P	0.046	0.986|0.012	0.965|0.017	18.41|0.003	0.972|0.023	0.456|0.019
5	Y_C-I-FP	0.049	0.768|0.328	0.792|0.277	18.81|0.288	1.069|0.124	0.407|0.197
6	Y_C-R-FP	0.042	0.984|0.011	0.966|0.017	18.40|0.002	0.977|0.026	8.4×10^3|0.6
7	Z_C-C-P	0.075	0.983|0.011	0.969|0.022	18.46|0.004	0.956|0.025	0.468|0.018
8	Z_C-I-P	0.050	0.973|0.128	1.070|0.095	19.07|0.272	1.075|0.085	0.400|0.154
9	Z_C-R-P	0.095	0.990|0.030	1.006|0.061	18.51|0.006	0.951|0.031	0.474|0.028
10	Y_C-C-FPO	0.276	0.925|0.096	0.339|0.110	···	0.731|0.008	0.502|0.008
11	Y_C-C-FPO	0.314	1.105|0.112	0.664|0.120	···	0.712|0.009	0.500|0.008

(3) to represent $EDAE_1$ response, and thus one fitting parameter is $\ln(r)$ rather than r itself. Because for actual data one will not know that $\phi_C = 1$, as it is here, it is important to include ϕ_C as a possible free parameter. The remaining parameters involved in the fit are $R(0)$, τ_∞, and C_B. For $r = 10^8$, $\ln(r) \simeq 18.420\,68$. Table II summarizes the results of numerous fits. Lines 1–9 show results of fitting the $EDAE_1$ model (free ϕ_C parameter) and DAE-box model (ϕ_C fixed at the value 1: lines 1 and 3) to the above admittance data. The last two lines are the results of fitting with the WW model (line 10) and the Davidson–Cole response function.[33] The first two lines use the 49-point data set while the others involve the 73-point set.

The estimates of $\ln(r)$ given in lines 1 and 2 indicate that no adequate determination of r is possible when Ω_{max} is appreciably less than r, although the estimates of the other parameters are excellent. On the other hand, when $\Omega_{max} \gg r$, as it is for the other fits, good estimates of $\ln(r)$ are indeed possible. Notice particularly that the estimate of $\ln(r)$ in line 4 and of C_B in line 3 are very close to their expected values, 18.42 and 0.4457, respctively. As one might expect, the estimates derived from separate real or imaginary part NLSQ fittings are generally appreciably poorer than those obtained using full CNLS fitting. In particular, the C_B estimate of line 6 is meaningless since the real part of the Y_C data is uninfluenced by the value of C_B. Although the imaginary-part fits of lines 5 and 8 yield generally adequate estimates, it was found that the NLSQ iterative convergence was very slow for these fits.

The results listed in lines 10 and 11 show that for the present data one can very well distinguish between right-model fits (lines 1–9) and some wrong-model ones. Furthermore, the wrong ones yield not only poor C_B estimates but also particularly misleading estimates of the relative standard deviation of this quantity. Detailed examination of the fits of lines 10 and 11 shows that the main part of the misfit arises here from the fitting of the real part of the data rather than from the imaginary part. The problem is that neither the WW nor the Davidson–Cole models involve any high-frequency cutoff and thus cannot well fit data derived from a more realistic model that incorporates such a cutoff and includes its effect. On the other hand, when the WW model, for example, is fitted to the 49-point data, where the cutoff is much higher than the highest frequency of the data so it does not affect the available response, one obtains a much better fit, one with an S_f only 45% larger than that of line 4. Nevertheless, even in this case, the difference is sufficient that one should be able to discriminate adequately between right and wrong models.

The foregoing results justify the following conclusions:

(a) The RFEB-CTRW box-distribution model has not been shown, as claimed, to yield significant quantitative agreement with electrical frequency response data for disordered solids or to be a particularly appropriate model for fitting such data.

(b) Complex nonlinear least-squares fitting of such data allows much greater model distrimination resolution than does complex plane or log-log plotting of the data.

(c) CNLS fitting has been shown to allow good discrimination between right and wrong models used to fit RFEB-CTRW box-distribution data containing random errors. Not only can the correct model be identified but such fitting with this model allows excellent estimates of its parameters and their uncertainties to be obtained.

(d) All decisions about goodness of fit of a model to data and about the most appropriate model for the data should be based on CNLS fitting of not just one, but of several possible models.

ACKNOWLEDGMENT

I much appreciate the financial support of this work by the U. S. Army Research Office.

[1] J. C. Dyre, J. Appl. Phys. **64**, 2456 (1988).
[2] J. C. Dyre, Phys. Lett. **108A**, 457 (1985).
[3] J. C. Dyre, J. Non-Cryst. Solids **88**, 271 (1986).
[4] J. C. Dyre, Phys. Rev. Lett. **58**, 792 (1987).
[5] J. R. Macdonald, J. Appl. Phys. **34**, 538 (1963).
[6] J. R. Macdonald, J. Appl. Phys. **58**, 1955 (1985).
[7] J. R. Macdonald, J. Appl. Phys. **58**, 1971 (1985). The $\exp(-N_{ii}E)$ term in Eq. (17) should be replaced by $\exp(-\eta_{ii}E)$ and the $\pm$ sign in Eq. (24) replaced by an equals sign.
[8] J. R. Macdonald, J. Appl. Phys. **61**, 700 (1987).
[9] J. R. Macdonald, J. Appl. Phys. **62**, R51 (1987).
[10] G. A. Niklasson, J. Appl. Phys. **62**, R1 (1987).
[11] M. Campos, J. A. Giacometti, and M. Silver, Appl. Phys. Lett. **34**, 226 (1979).
[12] C. De Dominicis, H. Orland, and F. Lainee, J. Phys. (Paris) Lett. **46**, L-464 (1985).
[13] E. W. Knapp, Phys. Rev. Lett. **60**, 2386 (1988).
[14] J. T. Bendler and M. F. Shlesinger, Macromolecules **18**, 591 (1985).
[15] J. Klafer and M. F. Shlesinger, Proc. Natl. Acad. Sci. USA **83**, 848 (1986).
[16] L. Borjesson, L. M. Torell, S. W. Martin, Changle Liu, and C. A. Angell, Phys. Lett. **125A**, 330 (1987).
[17] J. R. Macdonald and L. D. Potter, Jr., Solid State Ionics **23**, 61 (1987).
[18] J. R. Macdonald, Solid State Ionics **25**, 271 (1987).
[19] R. Becker and W. Doring, *Ferromagnetismus* (Springer, Berlin, 1939), p. 254.
[20] R. D. Andrews, N. Hofman-Bang, and A. V. Tobolsky, J. Polym. Sci. **3**, 669 (1948).
[21] A. V. Tobolsky, *Properties and Structure of Polymers* (Wiley, New York, 1960), p. 123f.
[22] H. Frohlich, *Theory of Dielectrics* (Clarendon, Oxford, 1949), pp. 93–95.
[23] K. Higasi, K. Bergmann, and C. P. Smyth, J. Phys. Chem. **64**, 880 (1960).
[24] A. Matsuomoto and K. Higasi, J. Chem. Phys. **36**, 1776 (1962).
[25] A. Rose, RCA Rev. **12**, 362 (1951).
[26] H. Fricke, Philos. Mag. **14**, 310 (1932).
[27] A. K. Jonscher, *The Universal Dielectric Response: A Review of Data and their New Interpretation*, Chelsea Dielectrics Group, Chelsea College, University of London (1978).
[28] J. R. Macdonald, Ed., *Impedance Spectroscopy-Emphasizing Solid Materials and Systems* (Wiley-Interscience, New York, 1987).
[29] J. Schrama, Ph.D. thesis, Leiden, 1957.
[30] R. L. Hurt and J. R. Macdonald, Solid State Ionics **20**, 111 (1986).
[31] J. R. Macdonald and R. L. Hurt, J. Chem. Phys. **84**, 496 (1986).
[32] J. R. Macdonald, J. Schoonman, and A. P. Lehnen, Solid State Ionics **5**, 137 (1981).
[33] D. W. Davidson and R. H. Cole, J. Chem. Phys. **19**, 1484 (1951).